Modelling Simul. Mater. Sci. Eng. 2 (1994) 913–920. Printed in the UK

An investigation of the back-scattering yield of Langmuir–Blodgett resist films in electron beam lithography

W Lu, N Gu, Z H Lu and Y Wei

National Laboratory of Molecular and Biomolecular Electronics, Southeast University, Nanjing 210018, People's Republic of China

Received 18 April 1993, accepted for publication 3 January 1994

Abstract. A 'refraction' model of a fast electron in multilayer media to describe the changes of the pathlength and the direction of the electron while it travels from one medium into another medium is proposed. Applying Monte Carlo techniques, the electron trajectories in Langmuir–Blodgett (LB) and spin-cast polymethylmethacrylate (PMMA) resists on an Si substrate covered with Cr films are simulated. The electron back-scattering yields in LB resists and spin-cast resists are calculated under different conditions. Finally, the superiorities of LB film resists in electron beam exposure lithography are discussed.

1. Introduction

Langmuir–Blodgett (LB) techniques enable transfer of a monolayer film on an air–liquid interface to a wafer [1]. The ultrathin, compact and uniform polymer films prepared by LB techniques, which are sensitive to electron beam and deep ultraviolet (UV) can be used as high-resolution resists (see, for example, [2] and [3]). As a kind of ultrathin resist, relative to conventional spin-cast resist films, the LB resist films have the advantages of low pinhole density, adequate etch resistance and ability to cover surface topography [4]. Besides these, the LB resist films have other advantages in electron beam lithography. In this paper, applying Monte Carlo techniques, we have simulated the electron trajectories and back-scattering yields in LB or spin-cast polymethylmethacrylate (PMMA) resist and substrate. From the electron back-scattering yields in LB and spin-cast resist films, we have evaluated the superiorities of LB resist films in electron beam exposure lithography.

2. Monte Carlo calculations

The basic computing model for the calculations of electron trajectories we adopted is similar to that used previously by other authors (see, for example, [5]–[7]). It is based on the following assumptions.

(i) Since the primary electron energy is much higher than the electronic binding energy in a solid, the interactions of the beam with the solid may be considered to be interactions with nearly free electrons and nuclei. The collisions between electrons and atoms may be adequately described by elastic screened Rutherford scattering from the nuclei. The differential scattering cross section, $d\sigma/d\Omega$, for scattering from the nucleus of an atom of atomic number Z is

$$d\sigma/d\Omega = Z(Z+1)e^4/16E^2[\sin^2(\theta/2)+\theta_0^2/4]^2 \qquad (1)$$

0965-0393/94/040913+08$19.50 © 1994 IOP Publishing Ltd

where E is the energy of the electrons, θ is the angle of scattering and θ_0 is the screening factor according to Nigam *et al* [8].

(ii) Since inelastic scattering only occurs through very small angles, we can assume that the electron direction is changed only by elastic scattering. According to the relation between collision parameter and differential scattering cross section [9], we can obtain

$$\sin^2(\theta/2) = \theta_0^2(1 - R_1)/(4R_1 + \theta_0^2) \tag{2}$$

where R_1 is a random number in the range $0 \leqslant R_1 \leqslant 1$.

(iii) The total scattering cross section obtained by integrating (1) through the full space is

$$\sigma = \pi Z(Z + 1)e^4/E^2\theta_0^2(1 + \theta_0^2/4). \tag{3}$$

Knowing the total cross section of a process allows us to give the length of a fast electron's mean free path in relation to that process. The mean free path between collisions is

$$\lambda = \left(\sum_i n_i\sigma_i\right)^{-1} \tag{4}$$

where n_i is the density of atoms of the ith species for a compound material and σ_i is its scattering cross section.

According to the theories of statistical physics, the mean free path obeys a Poisson distribution. The distance S an electron travels between collisions is

$$S = \lambda \ln R_2 \tag{5}$$

where another random number, R_2, is used.

(iv) Between collisions, electrons can be considered to lose energy continuously. So the energy loss per unit distance is governed by the Bethe energy loss relation [10]

$$\mathrm{d}E/\mathrm{d}S = -785(Z\rho/AE)\ln(1.166E/\bar{I})(\mathrm{eV}\ \text{Å}^{-1}) \tag{6}$$

where ρ is the density of the solid and I is its mean ionized energy, which is obtained semiempirically to be

$$I = \begin{cases} (9.76 + 58.8Z^{-1.19})Z & (Z \geqslant 13) \\ 11.5Z & (Z < 13). \end{cases} \tag{7}$$

In our calculations, the mean ionized energy of PMMA is

$$\bar{I} = (5Z_\mathrm{C}I_\mathrm{C} + 8Z_\mathrm{H}I_\mathrm{H} + 2Z_\mathrm{O}I_\mathrm{O})/(5Z_\mathrm{C} + 8Z_\mathrm{H} + 2Z_\mathrm{O}) \tag{8}$$

where Z_H, Z_C, Z_O are the atomic numbers of hydrogen, carbon and oxygen respectively and I_H, I_C, I_O are the corresponding mean ionization energies.

(v) For compound materials, for example PMMA, another random number R_3 is used to determine which atom in the solid acts as the scattering centre for the next scattering event. The probability per unit time for an electron of velocity v to collide with an atom of the ith species is [11]

$$\omega_i = n_i v\sigma_i. \tag{9}$$

Then the probability of scattering off an atom of the ith species using (9) is

$$P_i = (n_i\sigma_i)\left(\sum_i n_i\sigma_i\right)^{-1}. \tag{10}$$

If $R_3 < P_\mathrm{H}$, then a hydrogen atom acts as the scattering centre; if $P_\mathrm{H} \leqslant R_3 < P_\mathrm{H} + P_\mathrm{C}$, then a carbon atom acts as the scattering centre; finally, if $P_\mathrm{H} + P_\mathrm{C} \leqslant R_3$ an oxygen atom acts as the scattering centre.

However, in the above scattering model, the changes of pathlength and scattering angle have been neglected while electrons move from one layer into another. In fact, this assumption is not sufficiently accurate for a multilayer system. Within a medium, the electron step is usually equal to the pathlength, but special consideration must be used near an interface. In figure 1, supposing the present position of an electron in medium 1 is A, and the scattering angle is θ_1, computed by the Monte Carlo method, point O is the point of intersection between the line from point A along the electron's pathlength and the interface of media 1 and 2. When the computed pathlength S_1 extends past the interface between media 1 and 2, or $S_1 > \mathrm{AO}$, the electron enters a new medium, medium 2. If this is the case, then a new pathlength S_2 and a new angle θ_2 of scattering are computed under the same computing conditions as for S_1 and θ_1 except the medium. In other words, if medium 1 is the same as medium 2, then $S_1 = S_2$ and $\theta_1 = \theta_2$. Now according to the consistency of the scattering free path between two collisions, we have

$$\mathrm{AO}/S_1 + \mathrm{OB}/S_2 = 1 \tag{11}$$

that is

$$\mathrm{OB} = (1 - \mathrm{AO}/S_1)S_2. \tag{12}$$

Here, OB is the adjusted electron step in medium 2. The adjusted travelling direction in medium 2 is determined by computing the deviation angle $\Delta\theta$ between the refraction direction and OA, which is equal to $\theta_2 - \theta_1$. The next position B or B′ of the electron is determined by the sign of $\Delta\theta$. This satisfies the criterion that if medium 1 is the same as medium 2, then $S_1 = S_2 = S$, $\theta_1 = \theta_2 = \theta$, and $\mathrm{AO} + \mathrm{OB} = S$. In other words, in this situation, the travelling length is S and the angle of scattering is θ. This is identical to the single-medium situation.

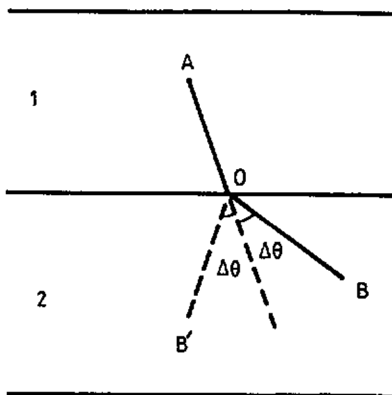

Figure 1. A refraction model for a high-energy electron in bilayer media.

Correspondingly, the electron energy E_B at point B is

$$E_\mathrm{B} = E_\mathrm{A} - \int_\mathrm{AO} \left(-\frac{\mathrm{d}E}{\mathrm{d}S}\right)_1 \mathrm{d}S - \int_\mathrm{OB} \left(-\frac{\mathrm{d}E}{\mathrm{d}S}\right)_2 \mathrm{d}S \tag{13}$$

where $(\mathrm{d}E/\mathrm{d}S)_1$ and $(\mathrm{d}E/\mathrm{d}S)_2$ are the energy loss rate in the first layer or the second layer respectively.

This 'refraction' model can be easily generalized to the situation where an electron passes through many layers within one scattering, shown in figure 2. Supposing an electron travelled from A_0 to A_i along the A_0A_1 direction in medium m_1. Its pathlength is S_0. Its energy at A_1 is E_1. Now we consider the situation where the electron travels through media $m_1, m_2, \ldots, m_{n-1}$ to m_n within one collision. We suppose the travelling lengths and the angles of scattering of the electron at point A_1 with energy E_1 in media $m_1, m_2, \ldots, m_n$ are $S_1, S_2, \ldots, S_n$ and $\theta_1, \ldots, \theta_n$ computed by (1)–(5).

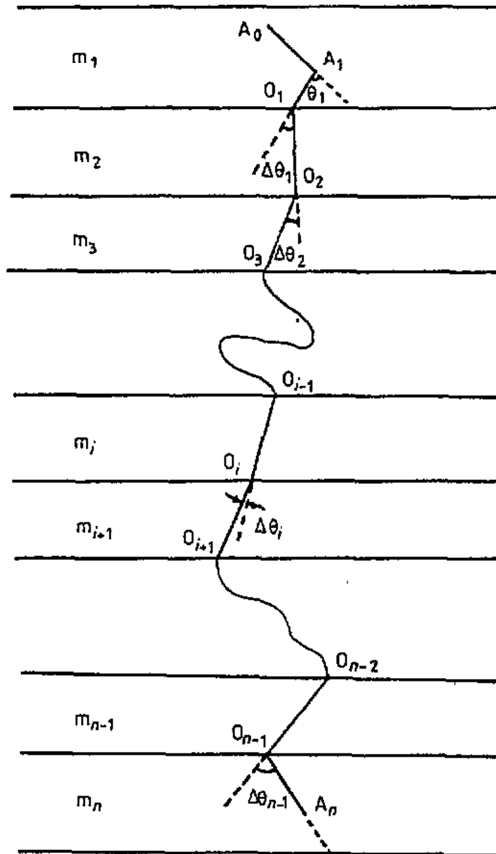

Figure 2. The refraction model for a high-energy electron in multilayer media.

In figure 2, $O_1, O_2, \ldots, O_n$ are the possible intersection points when the electron passes the interfaces within the scattering. The electron travels along the A_1O_1 direction at the beginning of the collision. If $S_1 > A_1O_1$, the electron will enter medium m_2. According to the above-mentioned method, we have

$$A_1O_1/S_1 + O_1A_2/S_2 = 1. \quad (14)$$

That is

$$O_1A_2 = (1 - A_1O_1/S_1)S_2 = (S_1 - A_1O_1)S_2/S_1. \quad (15)$$

The travelling direction of the electron in medium m_2 is determined by

$$\Delta\theta_1 = \theta_2 - \theta_1. \tag{16}$$

Now, supposing $O_1A_2 > O_1O_2$ gives

$$O_1O_2/S_2 + O_2A_3/S_3 = O_1A_2/S_2 \tag{17}$$

that is

$$O_2A_3 = (O_1A_2 - O_1O_2)S_3/S_2 \tag{18}$$

and similarly,

$$\Delta\theta_2 = \theta_3 - \theta_2. \tag{19}$$

Generally, if $O_{i-1}A_i > O_{i-1}O_i$, the electron will enter medium $i+1$. We can also define

$$O_{i-1}O_i/S_i + O_iA_{i+1}/S_{i+1} = O_{i-1}A_i/S_i \tag{20}$$

$$\Delta\theta_i = \theta_{i+1} - \theta_i. \tag{21}$$

The above calculations stop when $O_{n-1}A_n \leqslant O_{n-1}O_n$. Here, point O_n is the intersection of the extension line of $O_{n-1}A_n$ with the interface of medium n and medium $n+1$. At this time, the scattering within the n-layer medium ends. The energy of the electron at point A_n can be calculated by

$$E_n = E_1 - \int_{A_1O_1}\left(-\frac{dE}{dS}\right)_1 dS - \cdots - \int_{O_{n-1}A_n}\left(-\frac{dE}{dS}\right)_n dS. \tag{22}$$

Examining the above multilayer 'refraction' model, we have

(i) From (14)–(21), we can obtain easily

$$A_1O_1/S_1 + \cdots + O_{i-1}O_i/S_i + \cdots + O_{n-1}A_n/S_n = 1. \tag{23}$$

Obviously, if the media $2, \ldots, n$ are the same as medium 1, then

$$S_1 = S_2 = \cdots = S_n \qquad \Delta\theta_1 = \Delta\theta_2 = \cdots = \Delta\theta_n.$$

Therefore, in this case,

$$A_1O_1 + O_1O_2 + \cdots + O_{n-1}A_n = S. \tag{24}$$

This demonstrates that the model is coincident with the single-medium scattering model.

(ii) Obviously, in this multilayer 'refraction' model, the travelling length and direction of an electron in medium i are only relative to medium $1, \ldots, i-1$, and i. They have nothing to do with the other media.

(iii) In (14)–(20), the longer the pathlength S_i is, the larger the contribution of medium i for the total pathlength of a multilayer scattering is. That is, the total pathlength within one scattering increases with the increments of $S_1, \ldots, S_n$.

(iv) If the deviation angle $\Delta\theta_i$ is larger than the angle between the refraction direction of an electron and the interface i, the electron will go back into medium i. At this case, medium $i+1$ in the calculations will be the same as medium i.

To calculate the electron trajectories in LB PMMA film resists, we must determine the density and the number of atoms per unit volume in the LB PMMA film resist under the deposition conditions. The area per repeat unit under its deposition surface pressure can be acquired from the pressure–area isotherms of the PMMA LB film [12]. R F W Pease *et al* have measured that the thickness of a two-dimensional monolayer PMMA film on the subphase surface is 8.5 Å through ellipsometry [4]. So we can easily calculate the upper demanded parameters in our Monte Carlo calculations.

3. Computing results and discussion

To demonstrate the accuracy of the above-mentioned 'refraction' model, comparison experiments were performed. We calculated the back-scattering yields of electrons with 10 keV, 20 keV and 30 keV primitive energies incident on a GaAs substrate covered with 100 nm Al film using the general scattering model, which does not consider the changes of pathlength and direction in the multilayer film system, and using the above 'refraction' model. We have also performed electron back-scattering yield measurement experiments using a Hitachi scanning electron microscope (SEM). A Faraday cup, which is equipped to collect the electrons, is used to measure the total current of the electron beams. The electrons back-scattered from the specimen surface are captured and accelerated to bombard the plastic scintillator where they are converted into light. The light thus obtained is then fed to the photomultiplier after passing through the light guide and converted into an electric signal, which is then amplified by both the preamplifier and the main amplifier to be an intensity modulation signal of the electron beam. An Ohm contact, which is fabricated on the specimen, is connected to a preamplifier to measure the current of the electrons, which deposit their energies into the specimen. The back-scattering yields at different conditions can thus be obtained. The computed and experimental results are given in table 1.

Table 1. Comparisons of back-scattering yields computed by the two computing models and experimental results.

Method	10 keV	20 keV	30 keV
Monolayer	0.370	0.342	0.337
Multilayer	0.357	0.335	0.330
Experiment	0.352	0.331	0.319

It is well known that the back-scattering yield computed by the conventional scattering model is higher than the experiment data [10, 7]. From table 1, the results computed by the 'refraction' model achieved a better agreement with the experimental results. In other words, the multilayer medium 'refraction' model improved the computing accuracy. Besides, the specially designed electron beam lithography experiments on LB resist films and spin-cast resist films have verified the accuracy of the 'refraction' model [13].

Applying the above-mentioned model and the Monte Carlo method, we have simulated the electron scattering trajectories in LB PMMA resist and an Si substrate covered with Cr film. Figure 3 is the simulated trajectories in 100 Å LB PMMA and an Si substrate covered with 500 Å Cr film of 100 electrons with 5 keV primitive energy. The calculations followed the trajectory of an electron until its energy decreased below 500 eV.

In electron beam exposure lithography, the electron back-scattering yield in the resist and substrate is one of the key parameters because it reflects the proximity effect generated by electron-scattering interactions. We have calculated the back-scattering yields of electrons with different energies in LB PMMA resist and spin-cast films, as illustrated in figure 4. For accuracy in statistics, 2000 incident electrons were calculated for every condition.

From figure 4, relative to usual spin-cast resists, there is a smaller back-scattering yield in the LB resist under the same energy. In general, the factors to decrease the resolution because of back scattering in the electron beam exposure process are 10 times the factors for forward scattering. A smaller back-scattering yield reflects a smaller proximity effect. Therefore, the ultrathin LB resist preparation is an effective technique to lessen the proximity effect and to obtain high lithography resolution. In other words, in electron beam lithography, the use

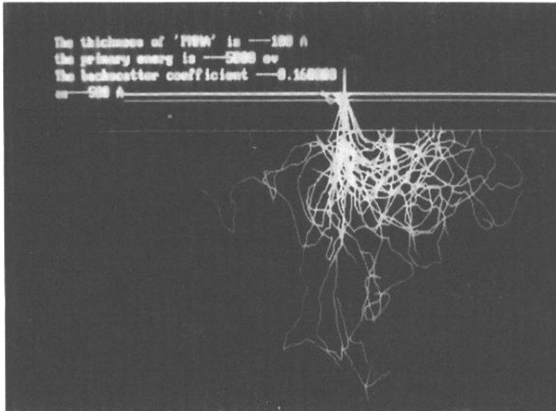

Figure 3. Simulated electron scattering trajectories in an LB PMMA resist and Si substrate covered with Cr film: primitive energy, 5 keV; LB PMMA thickness, 100 Å; Cr film thickness, 500 Å.

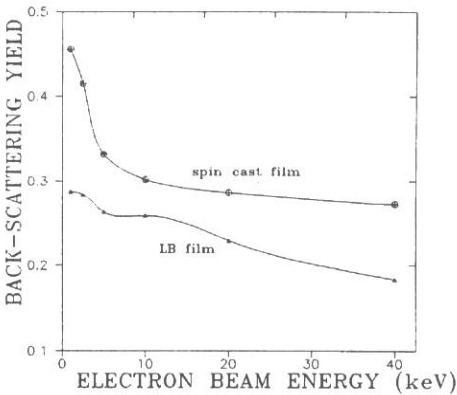

Figure 4. The curves of back-scattering yield of high-energy electrons in PMMA LB films and spin-cast films on an Si substrate. Here, the thicknesses of the LB films and spin-cast films are 100 Å and 5000 Å respectively.

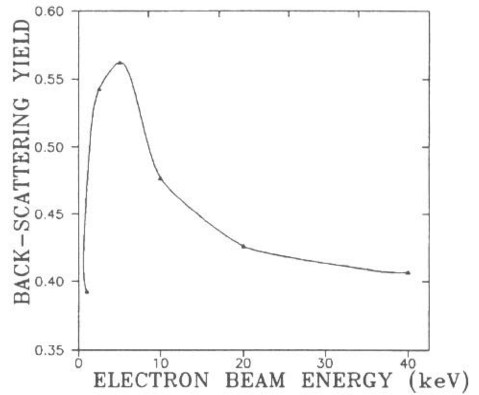

Figure 5. The back-scattering yield curve for 10 nm LB PMMA and Si substrate covered with 145 nm Cr film.

of LB resists will reduce electron scattering within the resists and thus make the proximity effect correction schemes easier to implement.

Figure 5 is the curve of electron back-scattering yield in an LB PMMA resist and Si substrate covered with 145 nm Cr film. For usual spin-cast resists, the higher the beam energy is, the smaller the back-scattering yield is generally. On the other hand, the simulation results demonstrated that lower energy ($\leqslant$ 5 keV) cannot let the electrons penetrate a 0.5 μm thick resist film to the substrate. However, from figure 5, there is a smaller back-scattering yield for both low beam energy and high beam energy for the LB resist. Comparing figures 4 and 5, we found that the back-scattering yield is higher for the substrate that consists of 145 nm thick Cr over Si at the same primary beam energy. This demonstrates that the high back-scattering yield can be reduced by using ultrathin resist films, by using a higher beam energy or by using a substrate consisting of a lower-atomic

number material. So we can potentially obtain high lithography resolution whether a high or low accelerating voltage is adopted for LB resist films. This makes ultrahigh-resolution photography practical even if we adopt a relatively simple electron beam exposure system, for example, modified SEM etc. Moreover, because the scanning tunnelling microscope (STM) can generate electron beams with a very low voltage and extremely high current density, the LB resist will allow electron penetration when the STM is used as an exposure tool. Because the STM is capable of creating ultrahigh-resolution patterns (better than 10 nm), it has become an important lithographic tool in nanofabrication in conjunction with the use of LB polymer films as resist materials.

4. Conclusions

We have demonstrated the improvements achievable using the 'refraction' expression to model the electron scattering in a multilayer medium system. This model provides a more accurate description of the scattering behaviours of a high-energy electron in multilayer media than does the conventional single-medium scattering model. From the results computed using the model, the following conclusions are drawn:

(i) for the same energy, the back-scattering yields for the LB resist are lower than those for the usual spin-cast resist;

(ii) there are lower back-scattering yields in LB resist films whether a low or high electron beam energy is adopted and

(iii) in electron beam lithography, the high back-scattering yield can be reduced by using ultrathin resist films, by using a high accelerating voltage or by using a low-atomic-number substrate.

Acknowledgments

This work was supported by the State Department of Electronic Industry under grant No 85-715-1-17.

References

[1] Blodgett K B 1935 *J. Am. Chem. Soc.* **57** 1007

[2] Calvert J M, Chen M S, Dulcey C S, Georger J H, Peckerar M C, Schnur J M and Schoen P E 1991 *J. Vac. Sci. Technol.* B **9** 3447

[3] Barraud A, Rosilio C and Ruaudel-Teixier A 1979 *Solid State Technol.* **22** 120

[4] Kuan S W J, Frank C W, YenLee Y H, Eimori T, Allee D R, Pease R F W and Browning R 1989 *J. Vac. Sci. Technol.* B **7** 1745

[5] Hawryluk R J, Hawryluk A M and Smith H I 1974 *J. Appl. Phys.* **45** 2551

[6] Liljequist D 1978 *J. Phys. D: Appl. Phys.* **11** 839

[7] Johnson S and MacDonald N C 1989 *J. Vac. Sci. Technol.* B **7** 1519

[8] Nigam B P, Sundaresan M K and Wu T-Y 1959 *Phys. Rev.* **115** 491

[9] Feldman L C and Mayer J W 1986 *Fundamentals of Surface and Thin Film Analyses* (Amsterdam: Elsevier)

[10] Bishop H E 1967 *Br. J. Appl. Phys.* **18** 703

[11] Rief F 1965 *Fundamentals of Statistical and Thermal Physics* (New York: McGraw-Hill) p 470

[12] Stroeve P, Srinivasan M P, Higgins G and Kowel S T 1987 *Thin Solid Films* **146** 209

[13] Lu W, Shen H Y, Gu N, Yuan C W, Lu Z H and Wei Y 1994 *Thin Solid Films* at press